LEGIBILITY NOTICE

A major purpose of the Technical Information Center is to provide the broadest dissemination possible of information contained in DOE's Research and Development Reports to business, industry, the academic community, and federal, state and local governments.

Although a small portion of this report is not reproducible, it is being made available to expedite the availability of information on the research discussed herein.

1

CONF-870581--11

LA-UR--87-2465

DE87 013165

TITLE: RADIATION-INDUCED TRANSIENT ATTENUATION OF OPTICAL FIBERS AT 800 and 1300 nm

AUTHOR(S): L. D. Looney, P-14
P. B. Lyons, ADDRA

SUBMITTED TO: SPIE,
Orlando, FL
May 20-25, 1987

RADIATION-INDUCED TRANSIENT ATTENUATION OF OPTICAL FIBERS AT 800 AND 1300nm

L. D. Looney and P. B. Lyons

Los Alamos National Laboratory
P.O. Box 1663, Mail Stop D410, Los Alamos, New Mexico 87545

Introduction

Radiation-induced absorption in optical fibers has been a subject of considerable interest throughout the world[1,2]. As availability and applications of fibers have evolved from "first window" systems operating near 850 nm to "second window" systems near 1300 nm, interest in wavelength dependence of radiation effects in optical fibers has similarly evolved. Several recent studies have explored second-window radiation effects with both steady state measurements[3,4] and, to a limited extent, with transient measurements[5]. No previous studies have explored the transient regime for times shorter than 10 μs.

The present work summarizes second-window, radiation-induced transient absorption measurements in optical fibers for times shorter than 5 μs. Comparisons to first window data for these fibers are also presented. Only high purity silica fibers with low-OH concentrations were used in the present study to avoid the large OH absorption band in this region.

This paper also collects first window data on several high-OH optical fibers. Preliminary data published previously[6] are confirmed for one specific fiber type.

Experimental Details

A Hewlett-Packard Febetron Model # 706 pulsed accelerator provided a 1.5 ns, 600 keV electron pulse after minor modification[7]. The fiber geometry was identical to that of ref. 8 and utilized a fiber length of 0.5-1.5 m in a single-layer coil of diameter less than 3.5 cm. The accelerator pulse was synchronized to a pulsed external light source.

Injection laser diodes (ILD) were used as light sources. For first window experiments, a Thomson ILD, type SE756, delivered 3 mw at 840 nm from its fiber pigtail. About 0.6 mw were present in the dosed region. A Hewlett-Packard 81589A receiver provided a dc-400 MHz frequency response with a sensitivity of 1 V/mw. For second window experiments, a Mitsubishi FU-31LD ILD provided 2.5 mw at 1280 nm from a fiber pigtail. A receiver of moderate bandwidth (65 Mhz) incorporated a RCA C30986-09C photodiode with response from 900 to 1500 nm.

A narrow band filter preceded the receiver and prevented excessive Cerenkov light from reaching the detector. Correction for Cerenkov light was nevertheless required, although this light persisted only during the short accelerator pulse. Particularly for the second window measurements, excess ILD noise complicated the measurements. This noise was greatly reduced by two techniques: rotation of the filter to prevent back-reflections into the ILD, and introduction of a mode scrambler at the fiber input. The latter technique was incorporated only for second window data and probably reduced modal instability problems arising where the narrow band filter was positioned. At this location the light was collimated, passed through the filter, and then refocused into a fiber pigtail on the receiver. The experimental layout is summarized in Figure 1.

Dosimetry was traceable to radiachromic films from Far West Technology, Inc. (Goleta, CA). These films provided calibration of a Farady cup current monitor in units of absorbed dose. Dosimetry details duplicated the procedure of ref 6. The Farady cup signal and the receiver outputs were recorded on Tektronix 7104 oscilloscopes over a wide range of sweep times. All absorbed doses are expressed in units of rads (SiO_2). Depth dose profiles were measured and are shown in Figure 2 together with the effective core regions for fibers tested herein.

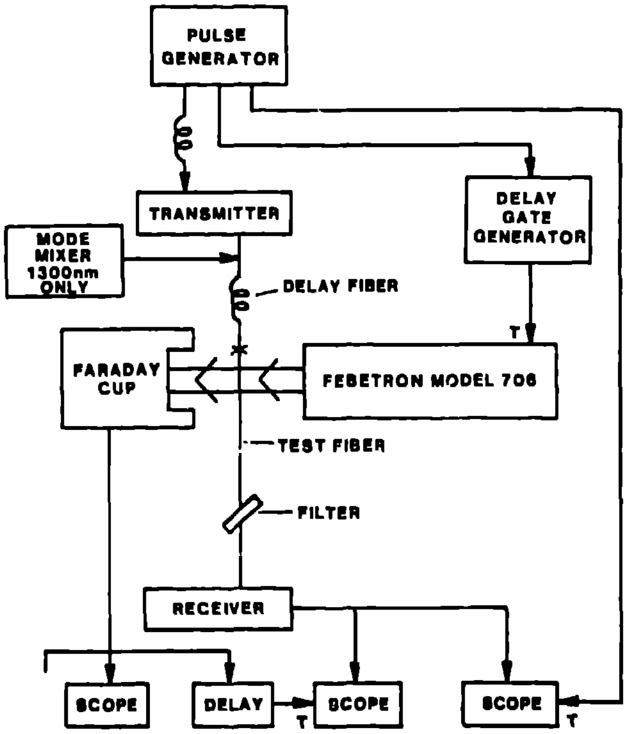

Figure 1. System schematic for the light injection, detection, accelerator, and recording system. Trigger inputs are denoted a T. All oscilloscopes were Tektronix type 7104.

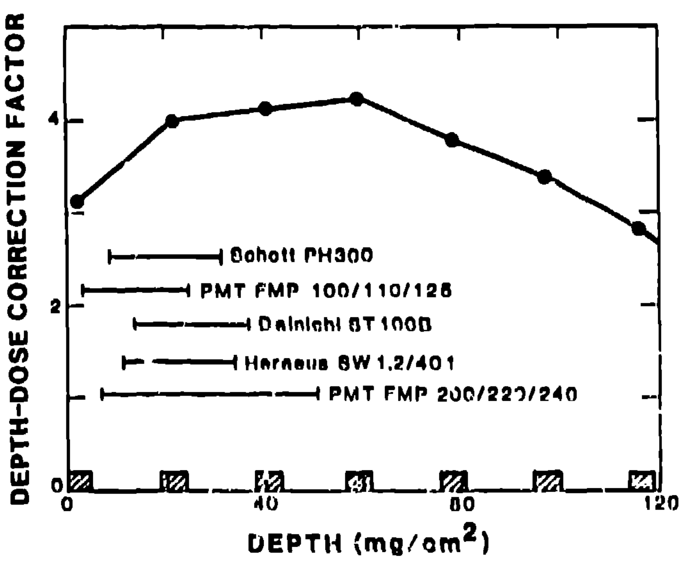

Figure 2. Depth dose distribution for the Febetron 706 experimental geometry. Along the horizontal axis, the cross-hatched areas identify locations of radiachromic films. The effective depths for the present fiber samples are shown on this figure.

Experimental Data

Low-OH Fibers

Radiation-induced transient absorption for four low-OH fibers was measured in both first and second windows. The four fibers were:

a) Dainichi ST100B fiber using a Diasil preform
b) Heraeus SW1.2/401 fiber using a Suprasil W preform
c) Schott P2347E from a plasma-impulse CVD preform[9].
d) A low-OH fiber from Poly-Micro Technology (PMT)

The first two fibers were part of a testing program coordinated under the auspices of a NATO effort.

Data are presented in two forms for the four fibers. In Figures 3-5, the dose-normalized transient absorption at 100 ns (in units of db/m-krad) is presented as a function of dose for both wavelengths. Distinction is made between predosed and new fiber in the figures. For the Heraeus fiber (b) data in Figure 4, predosed fiber show substantially greater damage. For the Dainichi fiber (a) in Figure 3, pre-exposure of the fiber causes little increase in induced absorption. In Figures 3 and 4, a strong nonlinearity is noticeable, with low dose leading to far greater damage. This phenomenon has been seen in all previous transient studies.

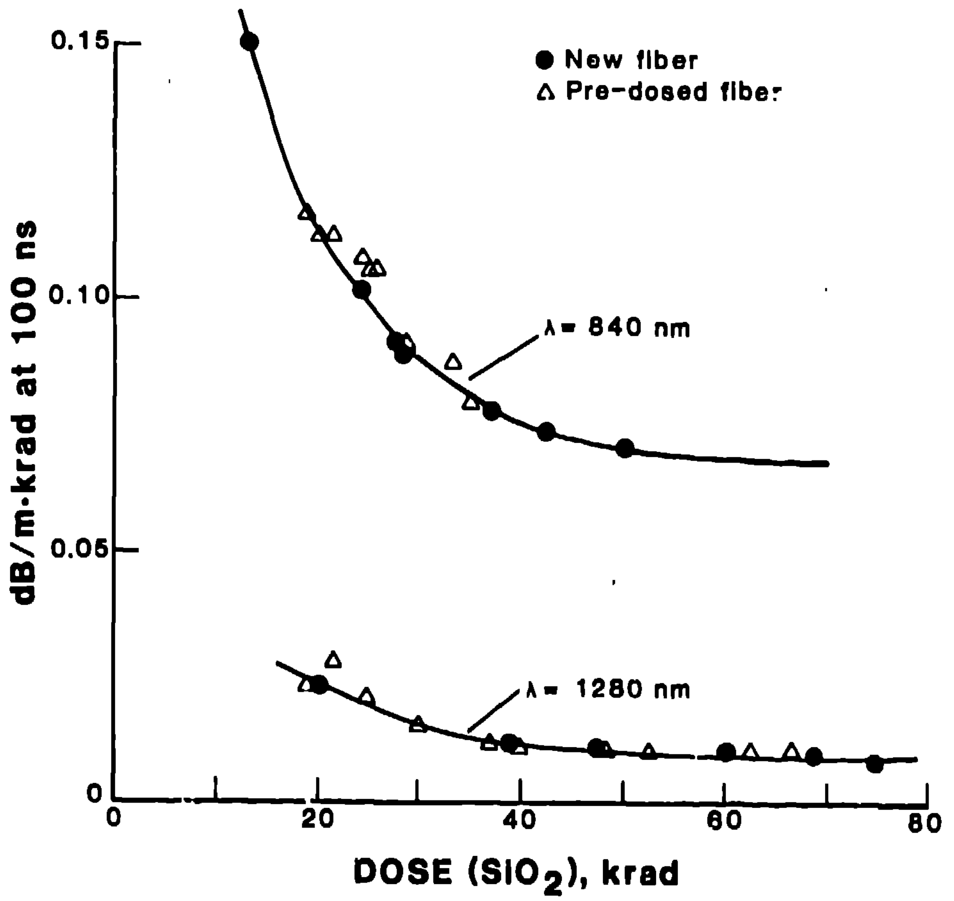

Figure 3. Transient attenuation of Dainichi ST100B optical fiber at 840 and 1280 nm wavelengths. The attenuation value measured 100 ns after exposure has been divided by dose for this presentation. Distinction is made between new and predosed fiber. Lines are intended only to guide the eye through data at each wavelength.

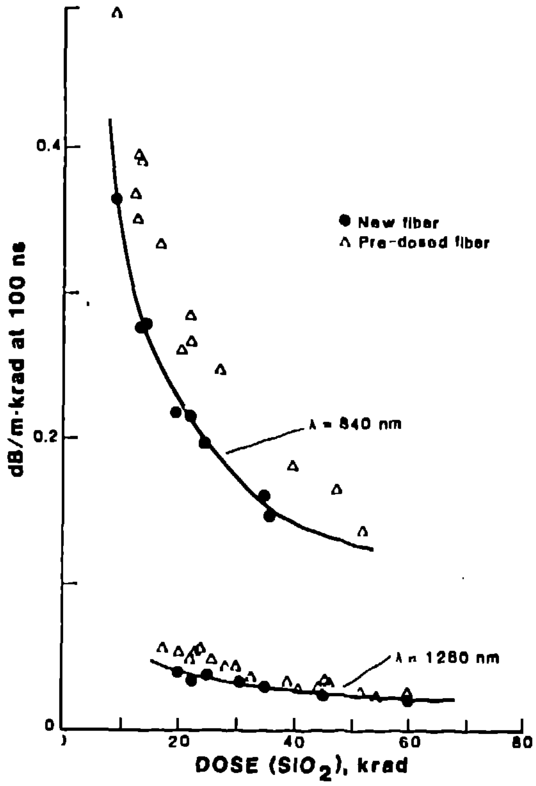

Figure 4. Transient attenuation of Heraus SW1.2/401 optical fiber at 840 and 1280 nm wavelengths. The attenuation value measured 100 ns after exposure has been divided by dose for this presentation. Distinction is made between new and predosed fiber. Lines are intended only to guide the eye through data at each wavelength.

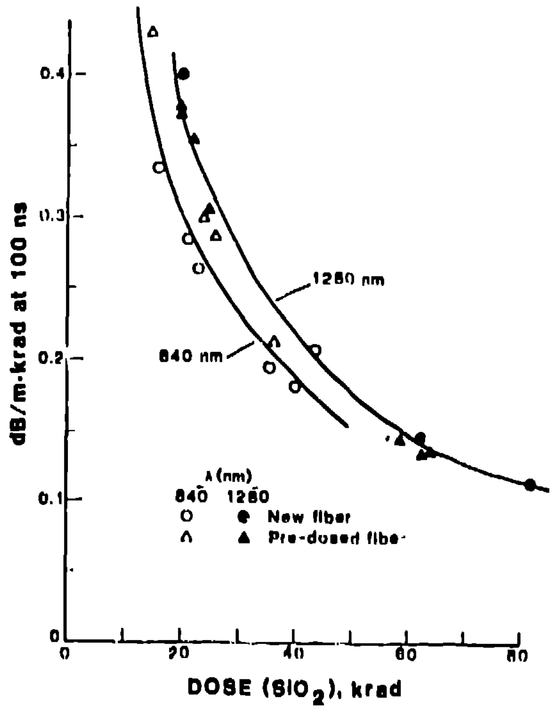

Figure 5. Transient attenuation of PMT 100/120/150 Low-OH optical fiber at 840 and 1280 nm wavelengths. The attenuation value measured 100 ns after exposure has been divided by dose for this presentation. Distinction is made between new and predosed fiber. Lines are intended only to guide the eye through data at each wavelength.

Figures 6 and 7 show induced absorption vs. time for fibers (a) and (b) for both wavelength windows and a range of doses. The figures were constructed through study of the transient absorption and recovery for the fibers as a function of time and dose. However, for all four fibers, no significant changes in the recovery dynamics were observed either for different doses or for predosed vs. new fiber. Thus, the recovery dynamics show no dose dependence in Figures 6 and 7. Figure 8 compares transient absorption for all four fibers at a single dose of 50 krad.

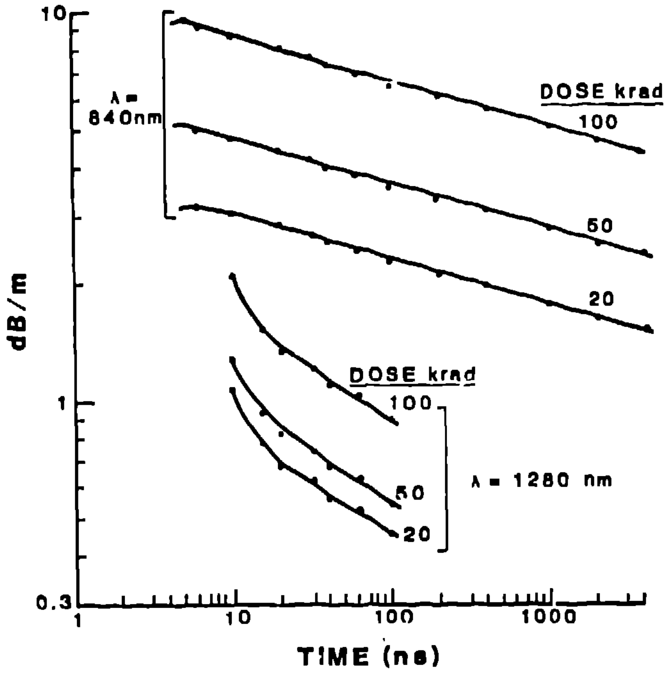

Figure 6. Transient attenuation vs. time for the Dainichi ST100B fiber at 840 and 1280 nm wavelengths. Dose is measured in kilorad (SiO_2). Lines are intended only to guide the eye.

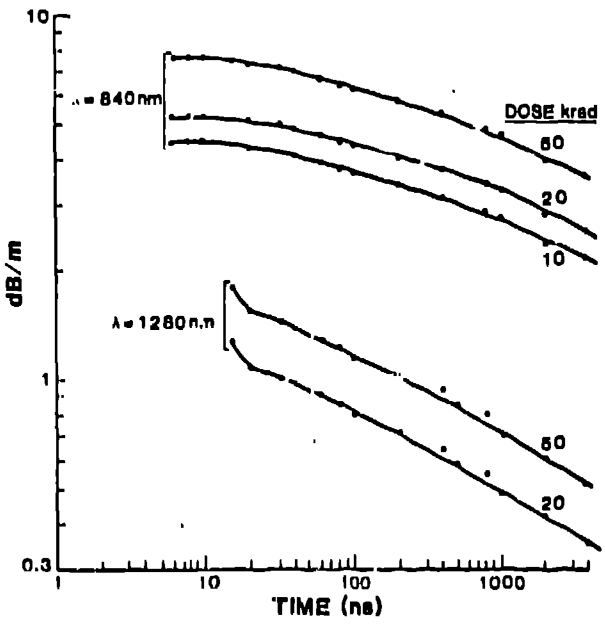

Figure 7. Transient attenuation vs. time for the Hereaus SW1.2/401 fiber at 840 and 1280 nm wavelengths. Dose is measured in kilorads (SiO_2). Lines are intended only to guide the eye.

A limited number of tests for second window data have been completed, leading to coverage of limited range of doses in the present data. Furthermore, the combination of reduced bandwidth receiver and low fiber absorption (which required long lengths of dosed fiber) precluded useful data for times below about 10ns for second window data.

Suprasil Core (High-OH) Fibers

In ref. 6, preliminary first window data for Polymicro Technologies (PMT) FHP 100 fiber were shown. At that time only a few data points were available for this fiber. Those early data showed very impressive radiation resistance. That fiber had a 100 μm core, a 110 μm cladding, 125 μm buffer layer, and was drawn from a Suprasil SSU preform.

Two additional PMT fibers have now been tested: another 100 μm core fiber with 110 μm cladding and 135 μm buffer layer; and a 200 μm core fiber with 220 μm cladding and 240 μm buffer layer. These data are collected in Figures 9 and 10, along with data for plastic-clad-silica (PCS) fiber from ITT that has been the subject of intensive previous study[7] and data for a fluorosilicate-clad Suprasil core fiber (Schott PH300) that has also been extensively studied (cf. ref 6).

Discussion of Data

Low-OH Fiber

Comparison of Figures 3-5 reveal major differences. In Figure 3 the Dainichi fiber exhibits significantly less damage at 1280 nm than the the other low-OH fibers fibers. This fiber also shows little, if any, difference between predosed and new fibers, suggesting essentially complete relaxation to the original conditions in the several minutes between electron pulses.

For both the Diasil and Suprasil W core fibers in Figures 3 and 4, the second window induced absorption is strongly reduced below the first window absorption. The data for the low-OH fiber in Figure 5, however, clearly demonstrate that this trend is not universally correct since, for this fiber, the trend is reversed. This latter fiber also exhibits more damage at both wavelengths than the Suprasil or Diasil fibers. The data in Figure 8 allow intercomparison of the four fibers for second window induced absorption with a dose of 50 krad. Large differences in recovery characteristics are evident for these four fibers. The Diasil core fiber presents the best performance for this group.

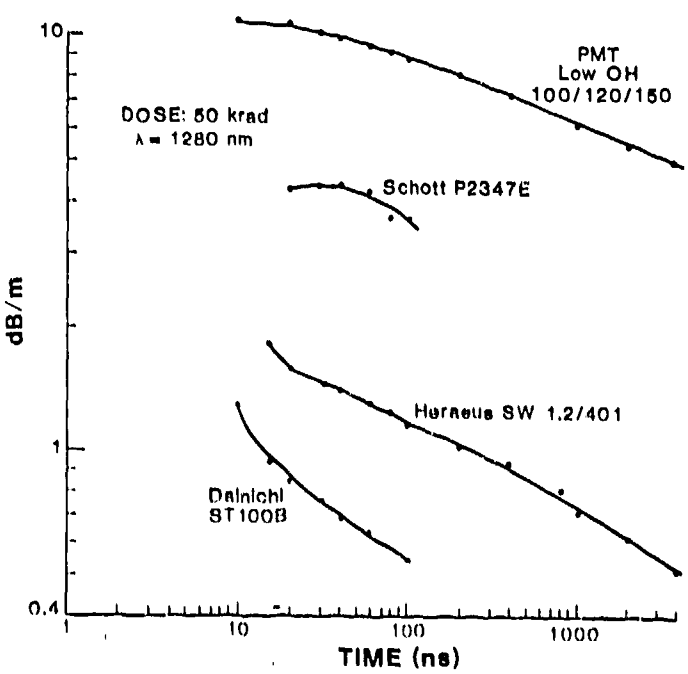

Figure 8. Comparison of transient attenuation for four fibers at 1280 nm.

High-OH Fibers

Figure 9 collects the first window induced absorption measured 100 ns after exposure and normalizes it bv dose. The two batches of PMT FHP 100 fiber display very similar performance, but that performance is not matched by the other three fibers. Ultraviolet transmission at 400 nm was documented by PMT for two of their fibers, yielding 26 and 40 db/km for the PMT FHP200/220/240 - and FHP100/110/135 fibers, respectively. Although low UV absorption in the 200 μm fiber might be expected to indicate a fiber with few defects and less radiation damage, Figure 9 does not support this hypothesis. One possibility for the inferior performance of the 200 μm core fiber would involve the higher stress in the larger core fiber as it was wound to the same coil dimensions as the 100 μm fiber. In the first window, these high-OH core fibers show much less damage than the low-OH fibers of Figures 3-5.

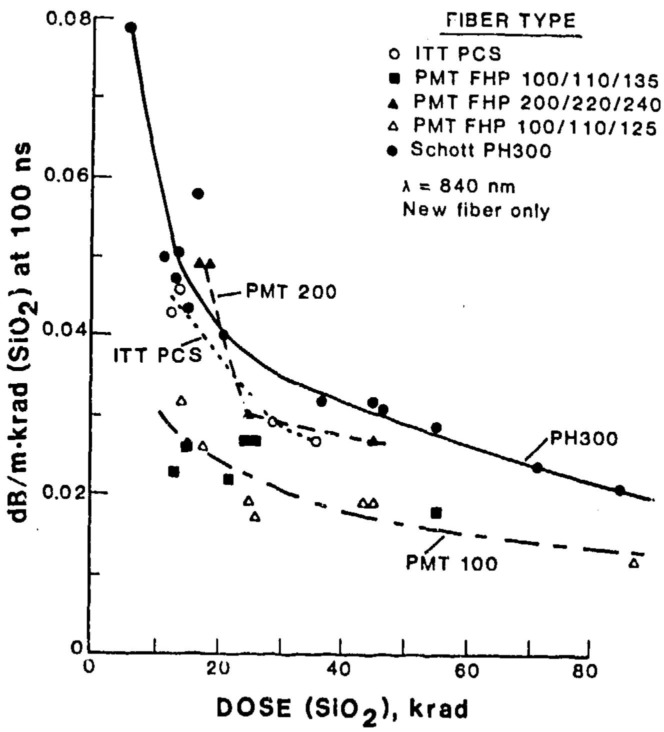

Figure 9. First window data at 840 nm for four fibers. Transient attenuation at a time of 100 ns after exposure has been normalized by dose and plotted as a function of dose.

In Figure 10, these Suprasil core fibers are compared for a fixed dose of 40 krad. While peak absorptions are quite similar, a slower recovery is evident for the large core PMT fiber, as well as the ITT-PCS and the Schott PH300. Two attributes of the PMT fibers may provide clues to their radiation resistance. Those fibers use Heraeus Type SSU preforms with a very thin clad layer, and this clad layer is uniformly doped. The Schott PH300 fiber used a Suprasil SS preform which provided flurosilicate clad glass in only a narrow cylinder around the Suprasil core. Most of the PH300 clad material was not flurosilicate. Furthermore, the PMT fiber is buffered with a polyimide coating, a process that requires high temperature application and could provide thermal annealing of defects. These observations, however, do not explain the observed difference between the FHP100 and and FHP200 fibers.

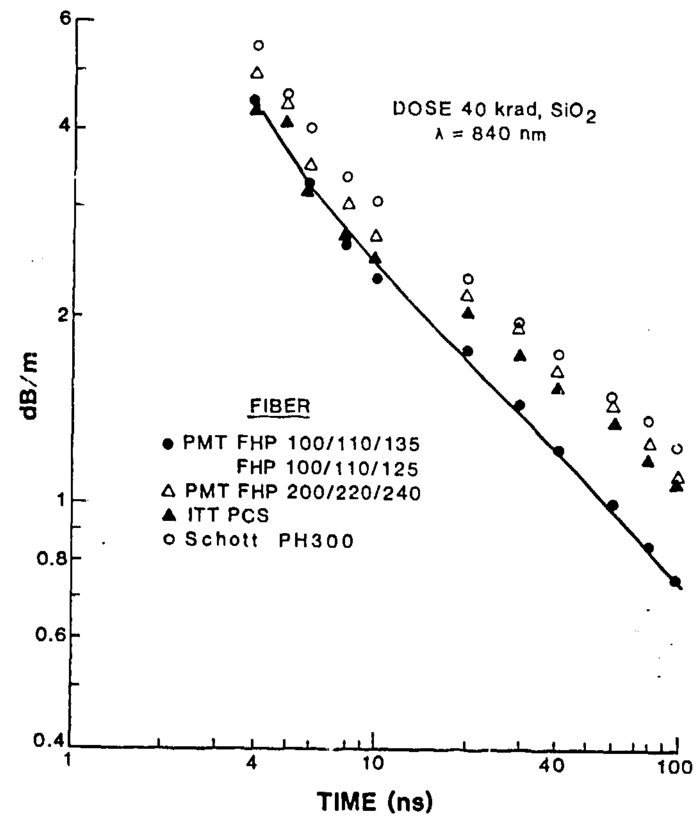

Figure 10. Transient attenuation vs. time for four fibers at a dose of 40 krad (SiO_2). Wavelength is 840 nm. The line is intended only to guide the eye through the data for the PMT FHP100 fiber.

Future Study

The second window data presented herein are slightly compromised by restricted receiver bandwidth. The data will be reacquired with an improved, higher bandwidth, receiver. The transient absorption of the 200 μm core PMT fiber will be studied as a function of coil radius to determine if core stress is degrading the performance.

Aknowledgment

The Heraeus SW1.2/401 fiber was provided by Dr. Klein of Heraeus Amersil. Dainichi ST100B was provided by Dainichi-Nippon. The PICVD fiber was provided by Dr. W. Schneider of MBB in Munich.

References

1. E. J. Friebele, C. G. Askins, M. E. Gingervich, and K. J. Long, "Optical Fiber Waveguides in Radiation Environments, II", Nucl. Inst. Meth. in Physics Research B1. p. 355. 1984.

2. P. B. Lyons, "Review of High Bandwidth Fiber Optics Radiation Sensors", SPIE Vol. 566, p. 166. 1985.

3. E. J. Friebele, K. J. Long, C. G. Askins, M. E. Gingerich, M. J. Marrone, J. Long, and D. L. Griscom, "Overview of Radiation Effects in Fiber Optics", SPIE Vol. 541, p. 70. 1985.

4. T. Suzuki, T. Hayashi, T. Gozen, H. Tanaka, and S. O. Kamoto, "Radiation Resistivity of Pure Silica Core Fibers", SPIE Vol. 721, p. 44. 1986.

5. W. Schneider, and V. Babst, "The Effects of Test Parameters on the Recovery of Febetron-Irradiated Optical Fibers", SPIE Vol. 721, p. 89. 1986.

6. L. D. Looney, P. B. Lyons, W. Schneider, and H. Henschel, "Influence of Preform Variations and Drawing Conditions on Transient Radiation Effects in Pure Silica Fibers", SPIE Vol. 721, 1986. p. 37.

7. L. D. Looney, G. Turquet de Beauregard, P.B. Lyons and R. E. Kelly, "Radiation-Induced Transient Absorption in Optical Fibers", SPIE 296, p. 17. 1986.

8. A. A. Hopkins, R. E. Kelly, L. D. Looney, P. B. Lyons, "Transient Attenuation in Optical Fibers", SPIE Vol. 506, p. 209, 1984.

9. H. VUXH, C. Paquet, W. Siefert, "Preparation of Optical Preforms by Plasma-Impulse CVD", SPIE Vol. 584, p. 33, 1985.